Journal of Oceanology and Limnology
Vol. 39 No. 3, P. 830-845, 2021
https://doi.org/10.1007/s00343-020-0149-8

Nitrate in the Changjiang diluted water: an isotopic evaluation on sources and reaction pathways*

Shan JIANG[1, **], Jie JIN[1], Guosen ZHANG[1], Yan CHANG[1], Zhaoru ZHANG[2], Meng ZHOU[2], Xiaolu WANG[1], Jing ZHANG[1, 2], Ying WU[1]

[1] *State Key Laboratory of Estuarine and Coastal Research*, *East China Normal University*, *Shanghai 200062*, *China*

[2] *School of Oceanography*, *Shanghai Jiao Tong University*, *Shanghai 200240*, *China*

Received Apr. 7, 2020; accepted in principle May 18, 2020; accepted for publication Jul. 14, 2020

Abstract A cruise covering two transects in the Changjiang (Yangtze) estuary in July 2017 was conducted, aiming to explore the sources for riverine NO_3^- and identify reactions involved in the NO_3^- transformations along the transport of the Changjiang diluted water (CDW). In the river water, NO_3^- was fundamentally contributed by chemical fertilizer leakage in the watershed according to isotope signals. Sewage discharge may also be significant on riverine NO_3^- inventory, while the isotope signal was masked by nitrification. Together with the transport of the CDW, NO_3^- production was observed in waters with low salinities (<20) and high turbidities. Nitrification resulted from the mineralization of riverine organic nitrogen; therefore, the high turbidity was linked to active production. In the outer plume, coupled with stratification, a significant decrease in NO_3^- concentration was observed in the surface water. In parallel, enrichment in $\delta^{15}N\text{-}NO_3^-$ and $\delta^{18}O\text{-}NO_3^-$ was found, indicating biological consumption by phytoplankton. The difference in the stratification intensity between two transects led to variations in NO_3^- concentrations and isotope compositions. In the benthic water, denitrification (sediment-water interface) and nitrification (bottom water) coexisted. Furthermore, accumulations of NH_4^+ and dissolved organic nitrogen in the bottom water were observed, indicating that nitrification was constrained by oxidant (mainly dissolved oxygen) supplies.

Keyword: Changjiang diluted water (CDW); denitrification and nitrification; estuary; production and removal; stable isotope

1 INTRODUCTION

Nitrogen (N) is essential in the biosynthesis of DNA, protein, phospholipid, etc., with global storage of 2.2×10^{10} Tg (Kuypers et al., 2018). Dissolved inorganic nitrogen (DIN) accounts for a small portion of total N inventory in the biosphere (Kuypers et al., 2018), but it is characterized by active cycling and transport. Biological and industrial nitrogen fixation introduces ca. 425 Tg N-DIN per year into the biosphere; while only 300 Tg N-DIN per year can be transformed to dinitrogen gas (Kuypers et al., 2018). Excessive DIN in terrestrial ecosystems, mainly nitrate (NO_3^-), is transported by surface rivers into coastal oceans through estuaries (47.8 Tg N/a; Galloway et al., 2004). The enrichment of land-borne NO_3^- in coastal waters frequently triggers harmful algae blooms and subsequent hypoxia, causing significant economic losses (Justić et al., 2003). Therefore, evaluating the magnitude of riverine NO_3^- fluxes and exploring the reaction pathways related with NO_3^- concentration variations in estuaries have received great attention from coastal managers and researchers (Wong et al., 2014; Loken et al., 2016; Yan et al., 2017; Domangue and Mortazavi, 2018).

The Changjiang River, length of ca. 6 300 km, delivers 9.24×10^{11} m^3/a river water to adjacent coastal oceans, ranking the fifth largest rivers on a global

* Supported by the National Natural Science Foundation of China (Nos. 41530960, 41706081) and the Scientific Research Foundation of SKLEC (No. 2017RCDW04)

** Corresponding author: sjiang@sklec.ecnu.edu.cn

scale (Milliman and Farnsworth, 2011). In the 1980s, the Changjiang delivered ca. 6.0×10^{10} mol NO_3^-/a to the East China Sea and the Yellow Sea (Edmond et al., 1985). Afterwards, the NO_3^- concentration in the Changjiang River water increased more than three folds, indicating a marked enhancement in river-borne NO_3^- input. Land-use changes due to rapid urbanization, overuse of fertilizers and sewage discharge are deemed to be key contributors of riverine NO_3^- (Dai et al., 2011). The Changjiang diluted water (CDW), consisting of the Changjiang River runoff and coastal saline water, could extend to more than 200-km distance from the river mouth and cover 10^4 km^2 surface area (31‰ isohaline; Chang et al., 2014). A series of research projects have been launched to explore the spatial/temporal distribution of riverine NO_3^- and reactions related to the concentration variation (Zhang, 1996; Yao et al., 2014; Yu et al., 2015; Liu et al., 2016; Yan et al., 2017). In the Changjiang estuary, nitrification, biological uptake, denitrification and anaerobic ammonium oxidation (Anammox) in the water column and/or benthic sediments have been determined (Song et al., 2013; Yan et al., 2017). These reaction pathways associated with NO_3^- addition (nitrification) and removal (Anammox, denitrification, assimilation, etc.) fundamentally influence NO_3^- concentration and the concentration-based impacts. Stable isotope compositions such as δ^{15}N-NO_3^- and δ^{18}O-NO_3^- are valuable for identifying reaction pathways of NO_3^-. In estuaries, mineralization of pelagic organic matter and subsequent nitrification decreases both δ^{15}N-NO_3^- and δ^{18}O-NO_3^-. In contrast, biological consumption leads to an increase in δ^{15}N-NO_3^- and δ^{18}O-NO_3^-. Theoretically, the ratio for the enhancement in δ^{15}N-NO_3^- and δ^{18}O-NO_3^- is 1:1 (Granger et al., 2010). Denitrification in the water column could produce a similar enrichment in δ^{15}N-NO_3^- and δ^{18}O-NO_3^-; while the enhancement in the isotope compositions caused by denitrification in the benthic sediment may not be observed if NO_3^- is fully converted (Yan et al., 2017). Accordingly, the combination of NO_3^- concentration and its stable isotope composition could improve our understanding of NO_3^- production and removal in the CDW.

Environmental factors in the Changjiang estuary, such as salinity, total suspended matter (TSM), and dissolved oxygen (DO), are highly dynamic because of the co-variation of tidal amplitude and the Changjiang River discharge rate, as well as stratification (Zhang, 1996). In addition, there are several outlets for the Changjiang River runoff (Fig.1). Discharge rates, tidal amplitudes, and related water residence time among these outlets are significantly different (Wu et al., 2010), which also deeply influences the related environmental parameters in the regions outside of these outlets. Biogeochemical reactions, including nitrification, denitrification, and assimilation are sensitive to the changes in these factors (Kuypers et al., 2018). Up-to-now, the published documents only revealed the variation of NO_3^- concentration and its isotope compositions in surface water (Liu et al., 2009) or on a single transect (Yan et al., 2017) in the Changjiang estuary. However, studies on NO_3^- distribution and reactions, as well as dynamic linkage between environmental factors and NO_3^- production/removal based on a comparison between multiple transects with different water depths are limited.

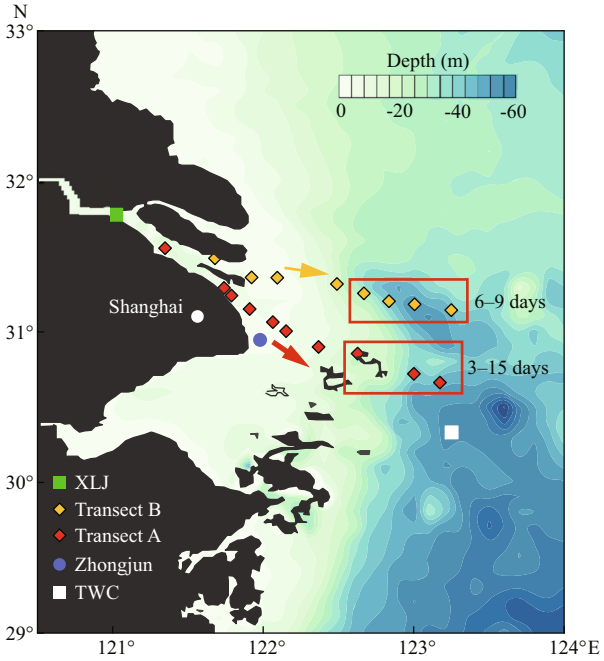

Fig.1 Sampling locations along two transects in the Changjiang estuary and Zhongjun station for the gauge of tidal amplitude

XLJ (Xuliujing) and TWC (Taiwan Warm Current) sites are also marked in the figure. Arrows indicate the cruise direction along two transects. Regions for diatom bloom on two transects are located in rectangles. Moreover, the water residence time in the rectangles ranged from 3 to 15 days and 6 to 9 days on both transects, measured by drifters at during the cruise.

In the present study, a cruise (R/V *Zheyuke II*) in the Changjiang estuary was conducted during summer 2017 when the Changjiang River discharge rate was high ($(6–7)\times10^4$ m^3/s gauged at Datong Station; http://www.cjh.com.cn). The objectives of this study were

(1) to identify NO_3^- sources in the Changjiang River runoff prior to river-sea mixing; (2) to determine reactions with regard to NO_3^- production and removal along the CDW pathway; and (3) to explore the relationship between the observed reaction pathways and environmental parameters, such as salinity, DO, and TSM in the estuary.

2 MATERIAL AND METHOD

2.1 Sample collection

The cruise in the Changjiang estuary was conducted on two transects (A and B) from 1st July to 8th July 2017, extending from river channels at the south branch (low salinity water) to the outer edge of the CDW as well as the Taiwan Warm Current (TWC) site (Fig.1). Besides, the river water at the Xuliujing (XLJ) site was obtained on 4th July 2017 (Fig.1). The tidal range gauged at the Zhongjun station (Fig.1) varied from 1.8 m on 4th July to 2.4 m on 8th July 2017. Transect A is the south outlet of Changjiang River runoff and adjacent to the deep-water channel, a channel for marine transport vessels. It has been surveyed in previous research projects related to NO_3^- transport and transformation (Wang et al., 2017; Yan et al., 2017). Transect B extends from another outlet with relatively high discharge rate. It is separated with transect A by the Changxing Island and Hengsha Island. During the survey, phytoplankton bloom (dominant species, *Skeletonema costatum*) was observed in the CDW outer plume on both transects (outlined in Fig.1). The water residence in these regions ranged from 3 to 15 days, estimated by drifters released in the river mouth at the beginning of the cruise.

Water samples during the cruise were collected from a CTD rosette sampler, equipped with 12-L Niskin bottles, a conductivity-temperature-depth (SBE 911, Sea-Bird Co.) unit and a fluorescence detector. In each site, 2–4 layers of the CDW, ranging from 3- to 53-m depth, were sampled. After collection, the measurement of DO concentration was immediately conducted using a detector (JENCO®, Model 9173). Approximately 1-L water was filtered through a polycarbonate membrane (pore size: 0.4 μm, Whatman®) for the quantification of dissolved nitrogen content, $\delta^{15}N\text{-}NO_3^-$ and $\delta^{18}O\text{-}NO_3^-$. The filtrate was stored at -20 °C until laboratory processing. Another fraction of water (0.3–3 L) was filtered by pre-combusted GF/F filter (average pore size: 0.7 μm, Whatman®). The solids retained on the filters were determined as the TSM concentration.

2.2 Laboratory analysis

Concentrations of DIN species (NH_4^+, NO_2^-, and NO_3^-) were determined on a flow injection analyzer (Skalar Analytical B.V., The Netherlands) using standard colorimetric procedures (Hansen and Koroleff, 1999). The method determination limit for these species was approximately 0.1 μmol/L. The analytical accuracy was approximately ±3%. The concentration of total dissolved nitrogen (TDN) was determined by the potassium peroxydisulfate ($K_2S_2O_7$) digestion method with the determination limit of 0.2 μmol/L and method precession of ±3% (Ebina et al., 1983). The level of dissolved organic nitrogen (DON) was obtained as the difference between TDN and DIN concentrations. The $\delta^{15}N\text{-}NO_3^-$ and $\delta^{18}O\text{-}NO_3^-$ were determined by bacterial reduction method (NO_3^- to N_2O, using *Pseudomonas aureofaciens*, Sigman et al., 2001) following the procedure described by Weigand et al. (2016). NO_2^- in samples was removed by the prepared sulfanilamide solution prior to bacterial reduction (Weigand et al., 2016). The generated N_2O was purified and concentrated in a Finnigan Precon System (Thermo Fisher, USA). Subsequently, N_2O and trace amount of CO_2 was separated by a chromatographic loop (GC Isolink; Thermo Fisher, USA). Afterwards, the $\delta^{15}N$ and $\delta^{18}O$ were analyzed in an isotope ratio mass spectrometer (Delta V; Thermo Fisher, USA). Measurements of $\delta^{15}N$ were referenced to atmospheric N_2 and $\delta^{18}O$ to Vienna Standard Mean Ocean Water (VSMOW) with standards of IAEA-NO-3, USGS-34, and USGS-35. The detection limit was approximately 1 μmol/L NO_3^- with the analytical precession of 0.2‰ for $\delta^{15}N\text{-}NO_3^-$ and 0.4‰ for $\delta^{18}O\text{-}NO_3^-$. The reproducibility of $\delta^{15}N\text{-}NO_3^-$ and $\delta^{18}O\text{-}NO_3^-$, based on long-run quality assurance tests, was ca. 0.22‰ and 0.51‰, respectively. The calibration of $\delta^{15}N\text{-}NO_3^-$ and $\delta^{18}O\text{-}NO_3^-$ was done according to Casciotti and McIlvin (2007).

2.3 Data analysis

Apart from the Changjiang River runoff, the Changjiang estuary receives seawater from the Taiwan Warm Current that intrudes into the estuary along 50-m isobath and the Kuroshio Current from East China Sea surface (Zhu et al., 2004). Kuroshio waters are oligotrophic (Zhang et al., 2007) while the TWC waters contain regenerated nutrients. Consequently, a three-endmember mixing model was developed to estimate water sources in the CDW

(identified by salinity and water temperature, Supplementary Fig.S1). Based on the identified water sources, calculation of the conservative distribution of NO_3^- concentrations, isotopic compositions, as well as NH_4^+ concentrations were conducted (more details in Yan et al., 2017). According to the difference in concentration or isotope compositions between the value derived from the model estimation and the observation, offsets for solute concentrations or isotope compositions were obtained. The positive offset for solute concentration indicates the production behavior, while a negative value is a mirror of removal. For isotope compositions, the positive reflects heavy isotope enrichment and vice versa. In the present study, the water parameters derived from the XLJ station (Fig.1), i.e. the upstream of both transects, were used to represent the Changjiang River water. For TWC water, the NO_3^- concentration and related isotope compositions, as well as NH_4^+ concentration were from the bottom of the southeast sampling site in the same cruise (Fig.1). For Kuroshio waters in the East China Sea, the NO_3^- concentration was obtained from Wang et al. (2016) and NH_4^+ concentration from Zhang et al. (2007). These values are outlined in Supplementary Table S1. Statistical analyses, such as regression and student's *t*-test, were carried out for the measurement of variables using Minitab 17.0 software (Minitab Inc., Pennsylvania State University). The significant level for all analyses was assumed to be α=0.05. The spatial distribution of parameters along each transect was plotted in Surfer 14.0 (Golden Software Inc., USA) and the dot plots were done in Sigmaplot 12.5 (Systat Software Inc., USA).

3 RESULT

3.1 Water chemistry parameters

Salinities of the cruise samples ranged from 0.11 to 34.5 on transect A (Fig.2a). On transect B, a similar range (0.13–34.4) was observed (Fig.2b). The salinity increased from the surface to bottom water. Additionally, the salinity difference between the surface and bottom increased from the river mouth to the outer plume, reaching ca. 8 due to strong stratification. The temperature of the Changjiang River surface water was approximately 26 ℃ and decreased to 18.9 ℃ at bottom water in the CDW outer plume (Fig.2c). TSM concentration in the estuary water ranged from 9.0 to 75.6 mg/L. On transect A, TSM rapidly increased in the salinities of 5 to 10 regardless of seawater dilution. Afterwards, the TSM concentration sharply decreased, dropping to approximately 10 mg/L at the outermost site. Fluorescence intensities, an indicator of phytoplankton biomass, ranged from 0.34 to 12.8 μg/L in the estuary water. On both transects, fluorescence intensities were low when water salinities <20. In the outer plume, fluorescence intensities rapidly increased and the watercolor darkened due to enrichment of phytoplankton, while the bottom water was fluorescence deficient (Fig.2g–h). DO concentrations were ca. 6 mg/L at the inner sites (all depth). In the surface water, the DO concentration gradually increased and peaked at the sites with high fluorescence intensity. When water depth increased, the DO concentration in the saline CDW dropped (minimum 3.9 mg/L) (Fig.2i–j).

3.2 N species and isotopes

NO_3^- was the major DIN species, and the concentrations of NO_3^- at the starting site (in the river channel) on transect A was approximately 119 μmol/L (Fig.3a). Together with salinity increases, NO_3^- decreased to ca. 5 μmol/L in the seawater surface (Fig.4a). On transect B, NO_3^- concentrations were ca. 108 μmol/L in river channels and dropped to 0.1 μmol/L in the outer plume (Fig.3b). At the starting site, NO_3^- concentrations in the surface and bottom waters were similar. The vertical difference in the NO_3^- concentration increased in the outer plume with enhanced stratification. In contrast to NO_3^-, NH_4^+ concentration in Changjiang River surface water was much lower (0.1–0.6 μmol/L). Concentrations of NH_4^+ increased to a maximum of 6.3 μmol/L at the higher salinity water (Fig.3c–d).

For the distribution of NO_2^-, its concentration on both transects was frequently below 1 μmol/L, indicating its instability (Fig.3e–f). The NO_2^- concentration showed a peak near the river mouth on transect A (Fig.3e), while no significant enrichment was found on transect B (Fig.3f). The DON level varied between 5.5 and 42.6 μmol/L. In the Changjiang River runoff (salinity <2), DON concentration was <20 μmol/L (Fig.3g–h). In the surface water on transect A (3–5-m depth), an increase in DON concentration, followed with decreases, was found. A similar peak in DON concentration was observed at the bottom of saline water (Fig.3g). On transect B, three DON concentration peaks were identified, mainly occurred in the bottom water (10–40-m depth) (Fig.3h).

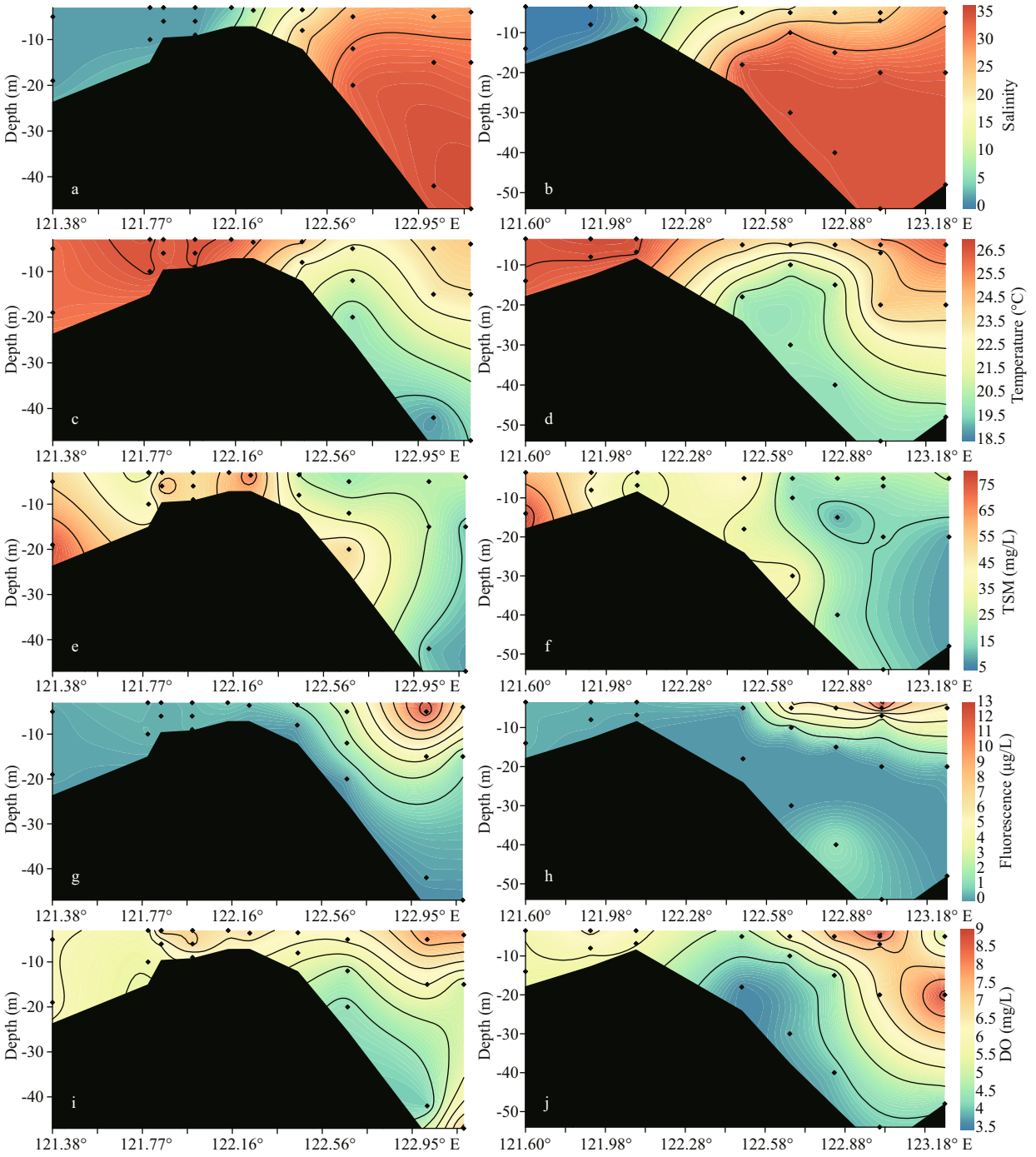

Fig.2 Profile of salinity (a & b), temperature (c & d), TSM (e & f), fluorescence (g & h), and DO (i & j) on both transects

The left panel shows the distribution on transect A while the right panel outlines the distribution on transect B. The profile extends from the river channel (ca. 121°E) to the CDW outer plume (ca. 123°E). The location of each site can be found in Fig.1.

Along transect A, $\delta^{15}N\text{-}NO_3^-$ ranged from 6.5‰ to 10.0‰ (Fig.5a). In the surface water, the elevation of $\delta^{15}N\text{-}NO_3^-$ along the salinity gradient from the river mouth to the offshore areas was observed (Fig.4a). In the outer plume of the CDW, $\delta^{15}N\text{-}NO_3^-$ decreased in the deeper water. The range of $\delta^{18}O\text{-}NO_3^-$ fell into -0.4‰ to 6.1‰ on transect A and displayed a similar trend along the salinity gradient as $\delta^{15}N\text{-}NO_3^-$ (Fig.5c). On transect B, $\delta^{15}N\text{-}NO_3^-$ in the Changjiang River runoff was 6.6‰. In the high salinity CDW, the surface water manifested a significant enrichment in heavy isotopes, reaching 17.4‰ for $\delta^{15}N\text{-}NO_3^-$ (Fig.5b). Nearly identical enrichment was found for $\delta^{18}O\text{-}NO_3^-$, peaking at 14.7‰ (Fig.5d). Unlike the

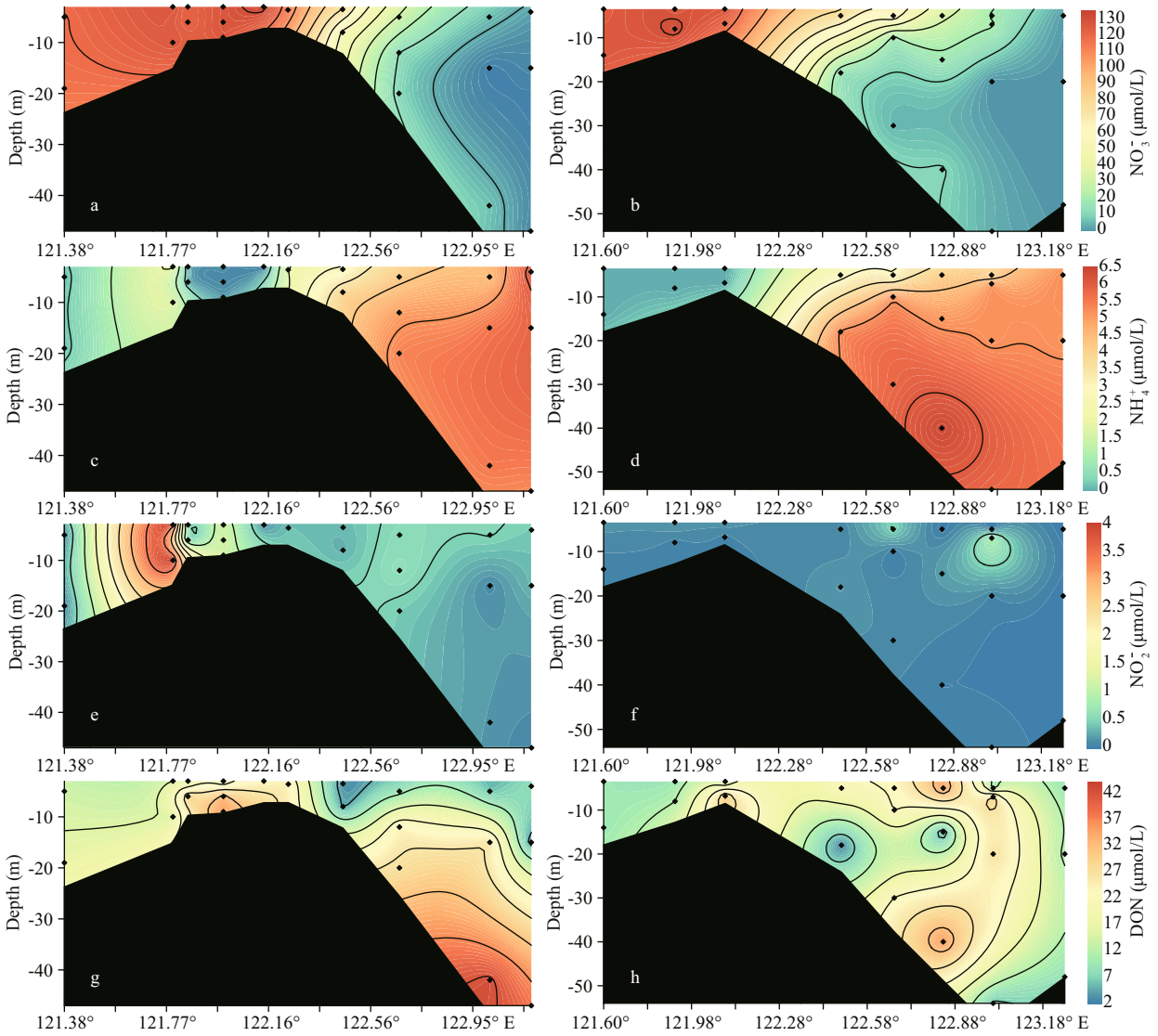

Fig.3 Profile of NO_3^- (a & b), NH_4^+ (c & d), NO_2^-, (e & f), and DON (g & h) on transect A (left panel) and transect B (right panel)

The profile extends from the river channel (ca. 121°E) to the CDW outer plume (ca. 123°E). The location of each site can be found in Fig.1.

surface water, both isotope compositions decreased in the bottom layers from the estuary toward the ocean. On both transects, positive correlations between $\delta^{15}N$/$\delta^{18}O$-NO_3^- and fluorescence intensity were observed (Fig.4c–d). For the correlation between isotope compositions and ln(NO_3^-) (natural logarithm of NO_3^- concentration), the surface and bottom water clearly separated into two clusters (Fig.4e–f), suggesting a stronger isotope fractionation in the surface water and regeneration in the bottom water. In addition, the slope of linear regression based on the surface water samples was large on transect B (Fig.4f).

3.3 Offsets for DIN and isotopes

The offset for NO_3^- concentration, i.e. the difference in NO_3^- concentration between the observed value and the values calculated from the three-endmember mixing model (Fig.6a), was outlined along the salinity gradient (Fig.6b, Supplementary Tables S2 & S3). On transect A, an increase in NO_3^- concentration offset was found at inner stations (high turbidity water). In the outer plume, the offset for NO_3^- concentration in the surface water was negative, suggesting an active consumption. The bottom water (high salinity) showed a patchy distribution and both increase and decrease in the offset values were obtained. Along transect B, offsets of NO_3^- concentration in low salinity water (ca. 0–20) were frequently smaller than values obtained from transect B. For NH_4^+ (Fig.6c), positive offsets were

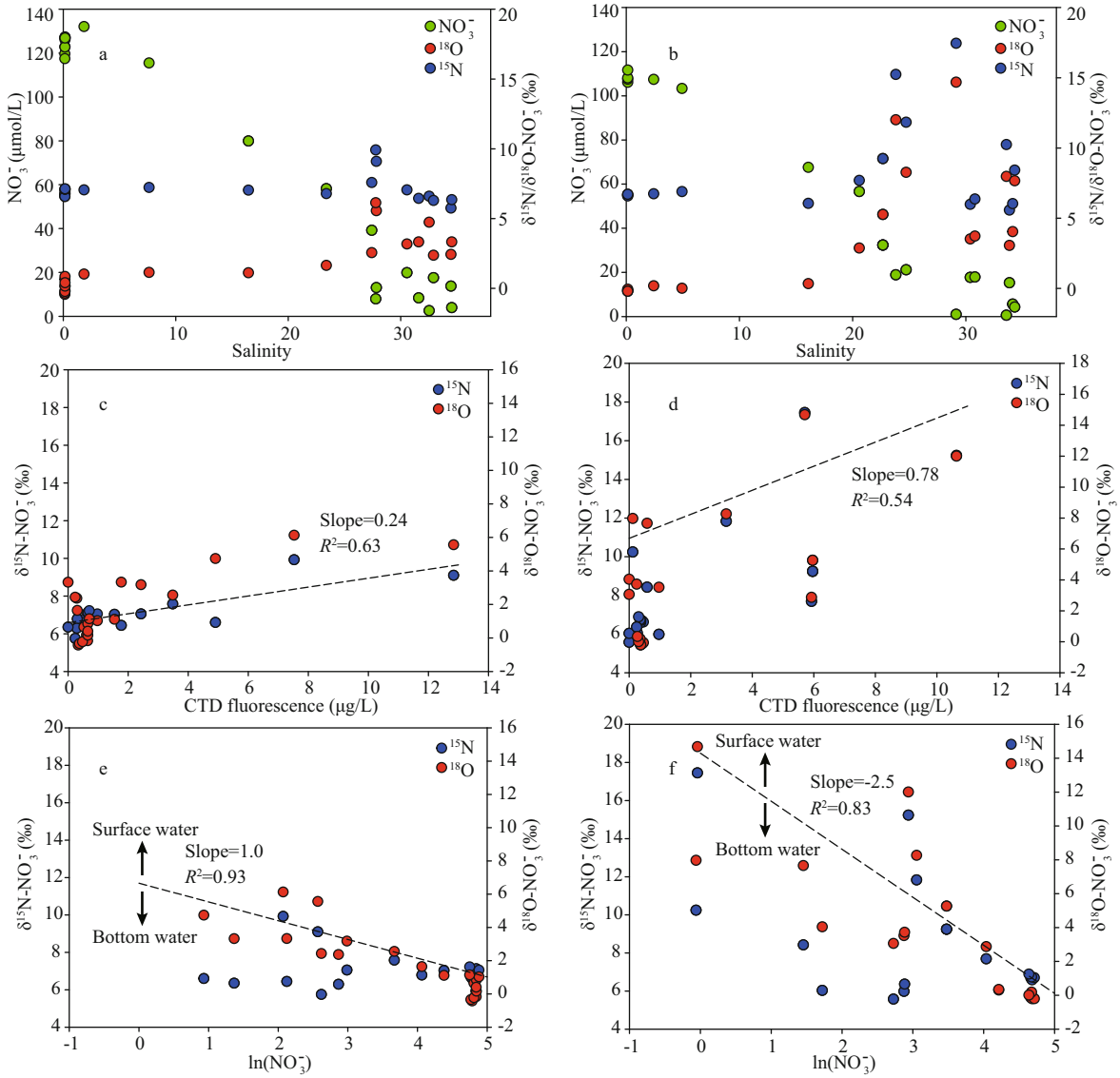

Fig.4 Correlations between NO_3^- concentration and isotope compositions with salinity (a & b); correlation between stable isotope compositions in NO_3^- and fluorescence (c & d), and NO_3^- concentration (logarithm, e & f)

Dash lines in c and d are regression between $\delta^{15}N\text{-}NO_3^-$ and fluorescence. Dash lines in e and f are regression of $\delta^{15}N\text{-}NO_3^-$ in the surface water. Left column was plots for transect A and right column was plots for transect B.

found in the outer plume, while negative values were observed in the low salinity water, especially on transect A. For isotope compositions, the water with the salinity below 20 showed a slightly positive offset for both $\delta^{15}N/\delta^{18}O\text{-}NO_3^-$ (Fig.6d–e). In high salinity water, a positive offset in the surface was found while it decreased dramatically in the bottom water. The linear correlation between $\delta^{15}N\text{-}NO_3^-$ and $\delta^{18}O\text{-}NO_3^-$ was significant (slope=1.22, R^2=0.90, P<0.05)(Fig.6f).

4 DISCUSSION

4.1 NO_3^- sources in the Changjiang River runoff

In the past forty years, NO_3^- concentrations in the Changjiang River runoff have markedly increased. At Datong station (600-km distance upstream of the first site on transect A), the NO_3^- concentration increased from ca. 30 to 120 μmol/L (cf. Fig.7a; data from Dai et al., 2011), accounting for the major component in the riverine DIN inventory (Fig.3a–b). In the current study, the NO_3^- concentration at the start of both transects (A: 119 μmol/L; B: 108 μmol/L) are comparable with published records from Yan et al. (2017). Enhanced NO_3^- inventory in the Changjiang River has been attributed to weak biological assimilation due to high turbidity (Zhang et al., 2007) and great contributions from multiple sources, including chemical fertilizer leakage from terrestrial

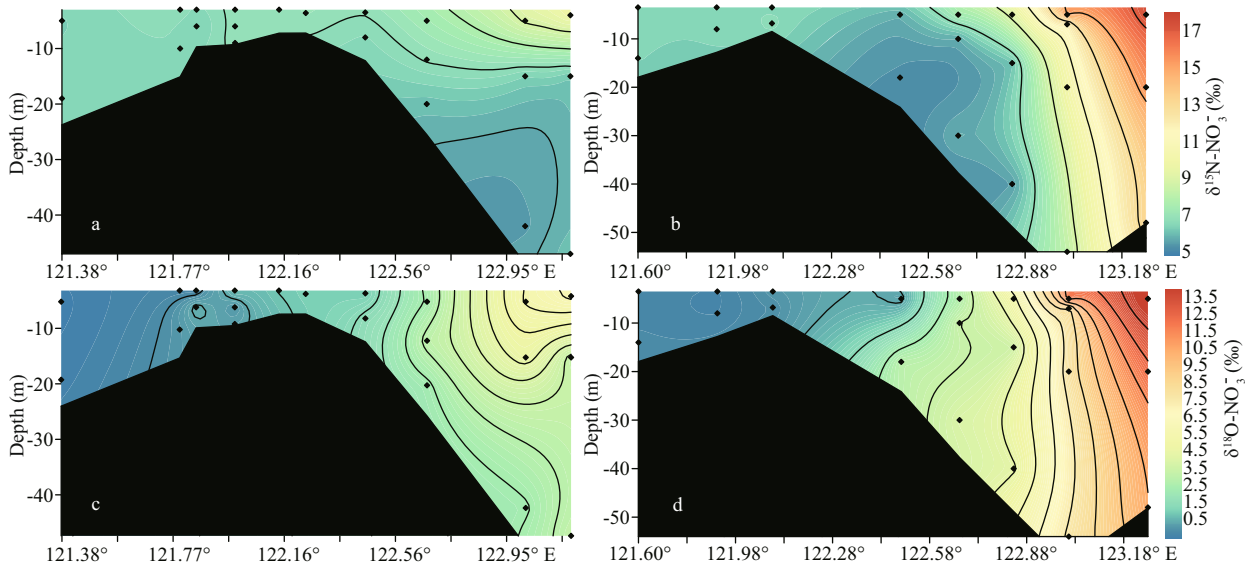

Fig.5 Profile of $\delta^{15}N\text{-}NO_3^-$ and $\delta^{18}O\text{-}NO_3^-$ on transect A (a & c) and transect B (b & d)

aquifers, wastewater discharge, atmospheric deposition and degradation of terrestrial organic nitrogen (Li et al., 2010; Dai et al., 2011).

Given the isotope compositions in the Changjiang River runoff (outlined in Fig.7b), both degradation of land-borne organic nitrogen ($\delta^{15}N\text{-}NO_3^-$: 4.5‰ to 7.5‰; $\delta^{18}O\text{-}NO_3^-$ <10‰) and leakage of chemical fertilizer ($\delta^{15}N\text{-}NO_3^-$: 0 to 7‰; $\delta^{18}O\text{-}NO_3^-$ <10‰) are likely to be important contributors (Chang et al., 2002; Li et al., 2010). In the Rajang River (Malaysia), the NO_3^- concentration was 7.6 μmol/L and the major source of riverine NO_3^- was the biological degradation of terrestrial organic matter due to the small population in its watershed (Jiang et al., 2019). In the St. Lawrence River (USA), another river with less anthropogenic disturbance, NO_3^- concentration was 30.4 μmol/L, lower than that of Changjiang River (Thibodeau et al., 2013). Consequently, the proportion of NO_3^- from organic matter decomposition may only account for a small portion in the riverine NO_3^- inventory. Instead, fertilizer leakage, especially NH_4^+/urea fertilizer, from terrestrial aquifers to the Changjiang River can be significant due to the intensive usage in agriculture to feed the large population. NO_3^- enrichments were also found in the Seine River (France), Zhujiang (Pearl) River (China) and River Thames (UK), where substantial chemical fertilizer was applied to support the large population in the watershed (Sebilo et al., 2006; Bowes et al., 2012; Cai et al., 2015). The temporal correlation between N fertilizer application amount in China and NO_3^- concentration in the Changjiang River water from the 1980s supported this conclusion (Fig.7a).

Interestingly, in the upstream of Changjiang River (Zhangjiagang), both $\delta^{15}N\text{-}NO_3^-$ and $\delta^{18}O\text{-}NO_3^-$ were 8.3‰ and 2.6‰, respectively (Li et al., 2010), which were comparable to sewage-borne NO_3^- enriched rivers, such as the Beijiang (China; Chen et al., 2009) and the Potomac River (USA; Pennino et al., 2016). In the river mouth, isotope compositions dropped. Such a significant decrease is likely due to active nitrification in the river water (Hsiao et al., 2014), which increases NO_3^- concentration while decreases $\delta^{15}N/\delta^{18}O\text{-}NO_3^-$ (Sanders et al., 2018). The branches of the Changjiang River at the downstream, such as the Huangpu River, cover several megacities (e.g. Shanghai, Suzhou, Hangzhou). Different with the Changjiang River water, the mean concentration of NH_4^+ was similar to that of NO_3^- in these branches (e.g. 1.4 mg/L for NH_4^+; 1.1 mg/L for NO_3^- in the Huangpu River, Yang et al., 2007), suggesting the sewage loading. Coupled with nitrification, the sewage related NO_3^- input from adjacent cities also requires attention from managers and stakeholders. In Fig.7c, a global comparison among several rivers subject to intensive human activities was made. Due to the relatively large discharge rate (9.24×10^{11} m^3/a; Milliman and Farnsworth, 2011), NO_3^- delivered from the Changjiang River is on the top of the list (Fig.7c), even the yield of NO_3^- in the entire watershed was much smaller than the Zhujiang River and the River Thames. Currently, the Chinese government puts substantial efforts into restoring the land cover in the watershed and reducing the application of fertilizer (Huang et al., 2008); therefore, a gradual reduction in the river-borne NO_3^- flux can be expected.

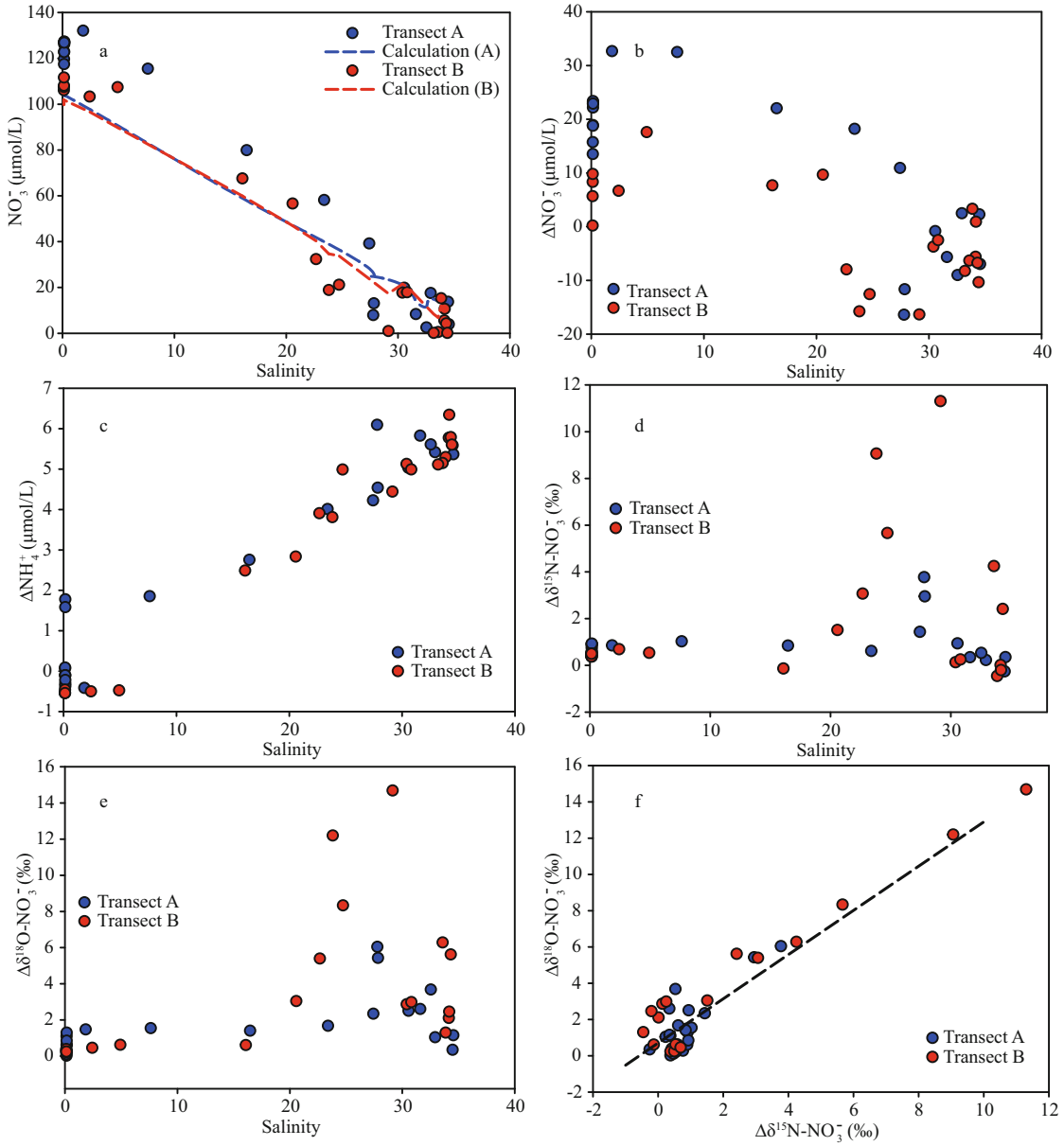

Fig.6 Difference between model calculated NO_3^- concentration (dash line) and observation value (points) (a); distribution of NO_3^- (b), NH_4^+ (c), $\delta^{15}N\text{-}NO_3^-$ (d), and $\delta^{18}O\text{-}NO_3^-$ (e) offsets (Δ in the figure) along the salinity gradient; correlation between $\delta^{15}N\text{-}NO_3^-$ and $\delta^{18}O\text{-}NO_3^-$ offsets (f)

4.2 NO_3^- production in the CDW

In the estuary, apart from potential errors introduced from sampling and irregular water mixing (e.g. small eddies), NO_3^- addition was found in salinity <20 (existing from the Changjiang River channels to the high turbidity water) and the outer plume (salinity >26), because of the positive offsets referenced to the conservative mixing status (Fig.6b). The increment in NO_3^- concentration at low/moderate salinity is in line with the findings reported by Liu et al. (2009) and Yao et al. (2014). The input from Changjiang River branches, especially the Huangpu River, to the Changjiang estuary might be the first reason for the increase. However, the NO_3^- concentration in the Huangpu River was lower than the level in the Changjiang River runoff (Yang et al., 2007). More importantly, compared with the Changjiang River discharge rate in summer ((6–7)×10^4 m^3/s), the Huangpu River loading was two orders of magnitude smaller (Zhu et al., 2018). Adding these together, the NO_3^- concentration increase may not be the product of inputs from Changjiang River branches. In addition, the weak adsorption potential of NO_3^- on particles in estuary water (Eyre, 1994) and limited variation in the adsorption-desorption balance from pH 5 to 9

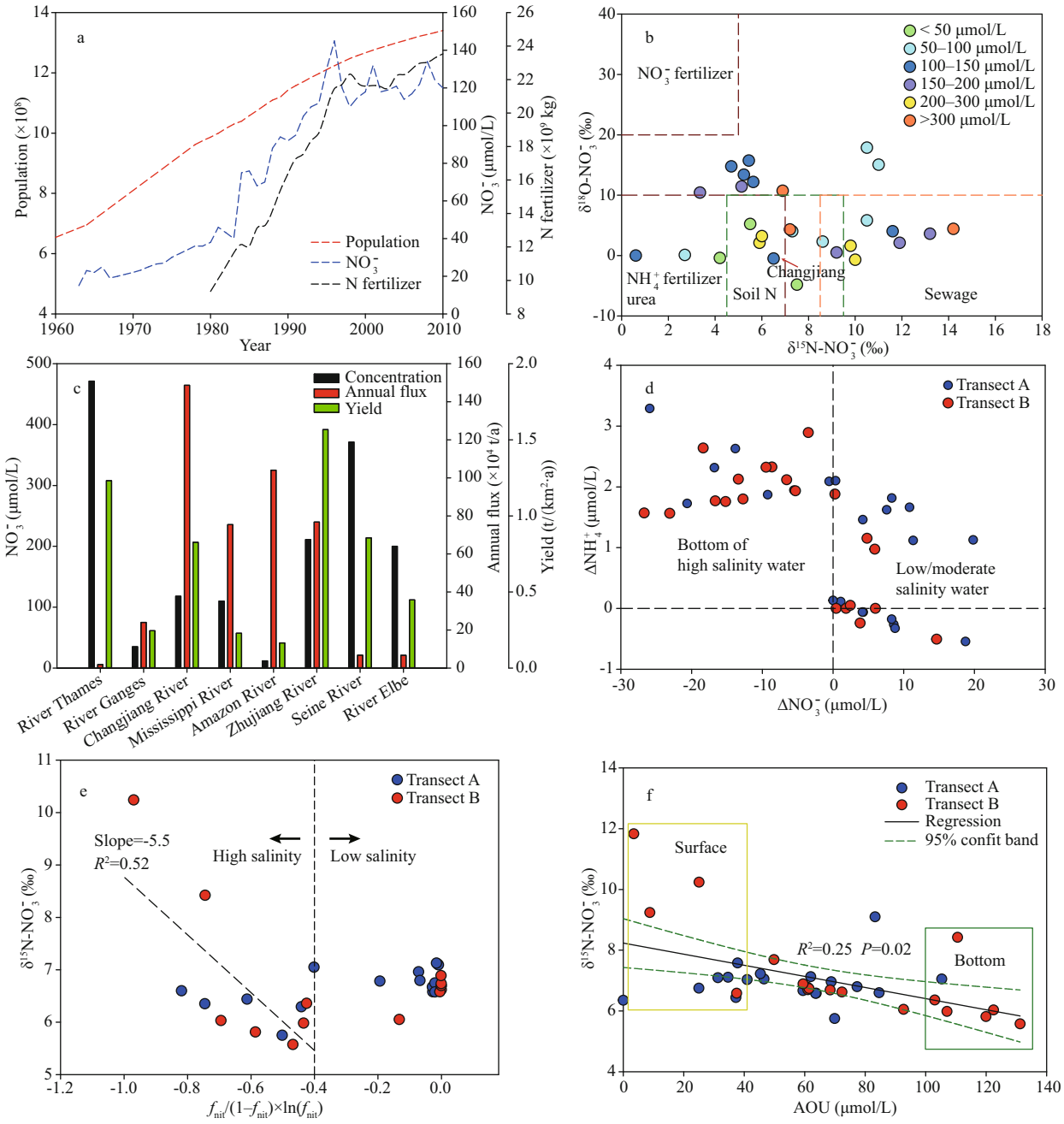

Fig.7 Growth of Chinese population and N fertilizer application (China National Bureau of Statistics, http://www.stats.gov.cn/) and NO_3^- concentration in Changjiang River water mainly determined at Datong Station (data mainly from Dai et al. (2011)) (a); distribution of $\delta^{15}N/\delta^{18}O$-$NO_3^-$ in river water before discharge to estuaries (salinity <0.5) on a global scale (b); comparison of NO_3^- concentration, annul flux, and watershed yield in different rivers on the global scale (c); correlation between NO_3^- concentration offset (Δ in the figure) and NH_4^+ concentration offset (Δ in the figure) in both transects (d); correlation of $\delta^{15}N$-NO_3^- in low salinity water (ca. salinity <20) and bottom of high salinity water (20–34) with $f_{nit}/(1-f_{nit})\times\ln(f_{nit})$ (e); correlation between $\delta^{15}N$-NO_3^- and AOU (apparent oxygen utilization) in the CDW (f)

In b, the isotope signals also highlight the potential sources for the riverine NO_3^-. The references of the displayed rivers can be found in Supplementary Table S4. The color used in the dot plots indicates the NO_3^- concentration in river water; in c, concentration data were obtained from Lohrenz et al. (1999), Sebilo et al. (2006), Santos et al. (2008), Bowes et al. (2012), Manna et al. (2013), and Cai et al. (2015). Annual discharge rate and area of the watershed were obtained from Milliman and Farnsworth (2011); in e, the dash line is the regression for the high salinity water.

(Zhang, 2007) indicate a minor influence from the adsorption-desorption process. Alternatively, the increase in NO_3^- concentration may result from intensive nitrification, as highlighted in Fig.8. On the one hand, the estuary directly receives riverine particles (Zhang et al., 2007) and microbes attached

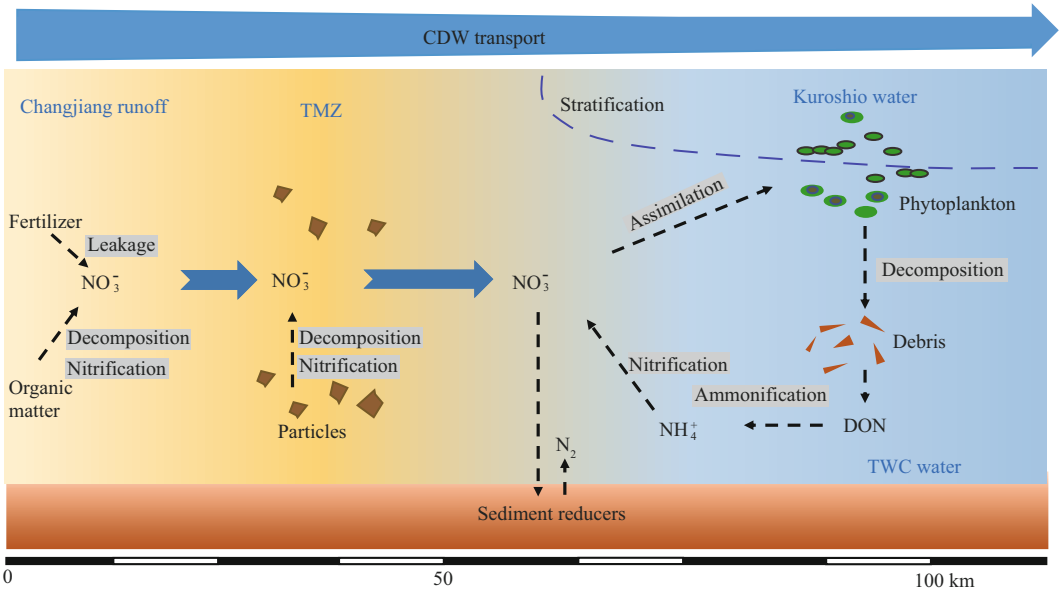

Fig.8 Sketch of NO_3^- addition and removal in the CDW with a description of reaction pathways and water masses from the current cruise

on particle surfaces. Given the high nitrification capability in the Changjiang River water, as aforementioned, it is not surprising to expect active nitrification on particle surface (Hsiao et al., 2014). On the other hand, seawater intrusion and desorption from the suspended particles, especially when salinity increases (Zhang, 2007), also add NH_4^+ for nitrification. Furthermore, TSM concentration at the freshwater endmember reached 55 mg/L. The proportion of N in TSM, measured by Gao et al. (2012) at XLJ, ranged from 0.12% to 0.24%, indicating a potential N source for NO_3^-. Moreover, an increase in DON content in the high turbidity water was observed, likely due to degradation from particles or desorption, which benefits NO_3^- production. For electron acceptors, DO was nearly saturated due to intensive mixing, which supported the transformation of organic N to NH_4^+ and eventually to NO_3^-. Notably, the variation in $\delta^{15}N$ in low salinity water was minor. In the Changjiang estuary, the reported mean $\delta^{15}N$ in suspended particle matter measured at XLJ was 5.1‰ (Zhang et al., 2007) and 6.2 ‰ (Gao et al., 2012), which were in line with the $\delta^{15}N$-NO_3^- value at the Changjiang River runoff (Fig.4a–b). This similarity supported the reaction chain that includes organic nitrogen mineralization and nitrification, especially on particles (Fig.8).

Intriguingly, between two transects, the concentration of NO_2^-, the intermediate product in the nitrification reaction chain, differed in the low/moderate salinity water. On transect A, the NO_2^- concentration peak was observed near the river mouth (Fig.3e), while an enrichment in NO_2^- was not observed on transect B (Fig.3f). Moreover, the peak value in positive NO_3^- concentration offset obtained on transect A (ca. 32 μmol/L) was higher than the value on transect B (17 μmol/L). Apart from the bias introduced from the endmember selection, reasons for these differences may be linked to the TSM concentration. In particular, on transect A, TSM concentration markedly increased from the river water to brackish water (ca. salinity <20) (Fig.2e), and a large area of turbidity maximum zone (TMZ) was observed by a turbidity probe equipped on a towed system during the cruise, mainly due to relatively low discharge rate and strong tidal swash. The location of TMZ on transect A fits the historical observation (Yang et al., 2015). The marked increase in TSM concentration likely stimulates nitrification by providing substrates for remineralization (a positive link between TSM and NO_3^- offsets in Supplementary Fig.S2). In addition, terrestrial particles in the TMZ were continuously suspended, prolonging the reaction time with oxidants, such as DO, in the water column. In contrast, a strong river plume rapidly injects and spreads in the East China Sea under the Coriolis force on transect B (Wu et al., 2010). Therefore, the typical TMZ along the transect was not captured during the cruise. Consequently, moderate NO_3^- generation was observed because the particle-dependent nitrification may have been influenced by low concentrations of TSM.

Elevations in NO_3^- concentration were also observed

at the bottom of high salinity water (e.g. A9 and B6 in Supplementary Tables S2 & S3). Due to wide coverage of permeable sediments, it is possible to assume that submarine groundwater discharge may have contributed to this increase. Given the high concentration of NO_3^- in groundwater, a small fraction could deeply change the NO_3^- concentration in the receiving water (Moore, 2010). Generally, contaminated groundwater was enriched in $\delta^{18}O\text{-}NO_3^-$ due to continuous denitrification (15‰ to 90‰), as summarized by Xue et al. (2009). Those values are significantly higher than the records obtained in the present study, indicating that the high concentration of benthic NO_3^- was not the result of groundwater injection. Alternatively, the increase in NO_3^- concentration was triggered by bottom water nitrification (Fig.8), which was supplied by the algae debris from the upper layer (Yan et al., 2017; Li et al., 2018). Compared to the nitrification rate in low salinity water, accumulation of NH_4^+ in the outer plume was found (Fig.7d). Nitrification is conducted by ammonia-oxidation archaea (AOA) and ammonia-oxidation bacteria (AOB) and the community structure in ocean water differs from that of terrestrial water (Martens-Habbena et al., 2009). Usually, the marine-derived AOA (the dominant contributor to nitrification) show a higher affinity to NH_4^+ (Kuypers, 2017), indicating active nitrification at the high salinity CDW (Hsiao et al., 2014). Given the positive linkage between nitrification rate and NH_4^+ concentration in the CDW (Wang et al., 2018), minor accumulation of NH_4^+ should be observed, which is against the current observation. Moreover, the $\delta^{15}N\text{-}NO_3^-$ fractionation was higher in the bottom of saline water than that in the low/moderate salinity CDW. In particular, the nitrification potential was introduced, which was defined as the slope between $\delta^{15}N\text{-}NO_3^-$ and $f_{nit}/(1-f_{nit})\times\ln(f_{nit})$, where f_{nit} is the concentration ratio between NH_4^+ and DIN (Wang et al., 2017). This potential in the water column is positively linked to nitrification produced NH_4^+ in the benthic waters under the same substrate condition. It also helps the identification of reactant sources for nitrification process. Clearly, the bottom water at outer plume showed a significantly positive correlation between $\delta^{15}N\text{-}NO_3^-$ and $f_{nit}/(1-f_{nit})\times\ln(f_{nit})$ (Fig.7e); whereas the trend in low salinity water was weak. The reason for such distribution can be attributed to the supply of oxidants. Near the river mouth, the shallow depth and extensive mixing lead to an active exchange of DO between the atmosphere and the estuary water. In the outer plume, stratification and enhanced water depth hampered DO exchanges, as evidenced by high values of apparent oxygen utilization (AOU) in the bottom water (Fig.7f). In the CDW, a linear correlation between $\delta^{15}N\text{-}NO_3^-$ and AOU was observed (Fig.7f), indicating the significance of DO in benthic nitrification. Furthermore, the suspended particles in the TMZ might contain high levels of trace metal, such as iron and magnesium, due to the adsorption and flocculation (Zhu et al., 2018). These metals could also act as the electron acceptor during nitrification (Hsiao et al., 2014); while the concentration is usually low in pelagic debris and saline water (Zhu et al., 2018). In summary, the DO supply and reactive trace metals constrained the nitrification rate in the bottom of saline water though reaction potentials can be high.

4.3 NO_3^- removal in the CDW

The NO_3^- removal appeared in two regions in the outer plume (Fig.8). In the surface water, turbidity decreased at seaward of the TMZ, which resulted from stratification, reduced turbulence and vertical mixing, benefiting the light availability for phytoplankton. It agrees with the observed phytoplankton bloom in the CDW front (Gao and Song, 2005). Hence, the NO_3^- consumption coupled with utilization by primary producers was observed, as depicted by the significantly positive correlation (R^2>0.54) between fluorescence intensity and $\delta^{15}N\text{-}NO_3^-$ (Fig.4c–d). In the present study, marked increases in NO_3^- isotope compositions occurred at the 20 isohaline (Fig.4a–b), which was identical to the value from Zhang et al. (2015) on $\delta^{30}Si$ enrichment in the estuary. Consequently, 20 isohaline can be treated as a starting boundary for the rapid uptake of nutrients by primary producers. As previously mentioned (Section 2.1), *Skeletonema costatum* was dominant in the outer plume on both transects. This assimilation increased isotope compositions, leading to strong correlations between NO_3^- concentration and $\delta^{15}N/\delta^{18}O\text{-}NO_3^-$ in surface water (Fig.4e–f).

Though with identical phytoplankton species, NO_3^- depletion (below 1 μmol/L) was observed on transect B (Fig.4b). In comparison, approximately 5 μmol/L NO_3^- still existed at the surface of transect A. Moreover, the correlation slopes of $\delta^{15}N/\delta^{18}O\text{-}NO_3^-$ to $\ln(NO_3^-)$ in the surface water were higher on transect B (Fig.4f), indicating strong isotopic fractionation during the consumption of NO_3^-. The surface water is usually limited in denitrification carriers due to high DO

content (Wong et al., 2014). Moreover, the fluorescence intensity and water residence time on both transects were similar. Adding these together, the difference in the stable isotope composition between transects A and B in this study likely results from strong stratification outside of the TMZ. The potential energy anomaly, an indicator of stratification, displays a peak on transect B (Supplementary Fig.S3), indicating a slow water exchange between the surface and bottom. Such strong stability is beneficial for the growth of phytoplankton in the surface water, which may have resulted in the continuous utilization of NO_3^- and elevation of $\delta^{15}N/\delta^{18}O\text{-}NO_3^-$ in the CDW plume. Interestingly, the enhanced NO_3^- utilization by *Skeletonema costatum* did not trigger a significant increase in biomass, as outlined by the similar CTD fluorescence intensity between transects A and B (Fig.2g–h). One reason is that strong currents in the Changjiang River plume had flushed the phytoplankton offshore. More importantly, this phenomenon may be linked to density effect, which suggests that algae concentration could not continuously increase; whereas algae communities, especially for the nutrient-sensitive species, such as *Skeletonema costatum* (Li et al., 2018), could continuously accumulate nutrient from ambient environment into cells (luxury consumption). Collos et al. (1992) revealed that intracellular accumulation of NO_3^- in *Skeletonema costatum* reached 17 mmol/L, i.e. several orders of magnitude higher than the ambient NO_3^- concentration. The excess N may be stored in the vacuole of the algae as amino acids or protein (Ketchum, 1939). When N concentration in the ambient environment decreases, the stored N could sustain the cell function and algae biomass, leading to a continuous bloom in the CDW. In the benthic water, decrease in NO_3^- concentration was also observed (Fig.3a–b). The concentration decrease mainly results from denitrification since *Skeletonema costatum* cannot actively move to the bottom water due to lack of flagellates (Li et al., 2018). Denitrification could occur in both the water column and sediments (Yan et al., 2017). Usually, 2 mg/L DO concentration was assumed to be the highest level that denitrifiers could bear in seawater (Codispoti and Christensen, 1985). The DO concentration in the present study was higher than this threshold. Therefore, sediments are the major rector for denitrification. In the Changjiang estuary, high denitrification potential in benthic and intertidal sediments, especially in cohesive sediments (muddy sediment), has been reported (Song et al., 2013). Coupled with exchanges between sediment porewater and overlying water, a significant fraction of NO_3^- was injected into sediments, especially the permeable sediments. Compared with the biological assimilation, denitrification in the sediment may not significantly alter stable isotope values (<0.5‰ here) because of the completed transformation (Yan et al., 2017). Moreover, sediment denitrification might be coupled with nitrification (Fig.8), effectively removing the produced NO_3^- and hence preventing the transport of NO_3^- from the deep water to surface water.

5 CONCLUSION

In the present study, the source of NO_3^- in the Changjiang River runoff before the river-sea mixing was mainly attributed to inputs from chemical fertilizer (based on $\delta^{15}N/\delta^{18}O\text{-}NO_3^-$ values), indicating the importance of management on fertilizer application and reforestation in the watershed. Sewage-related NO_3^- may also be important to the riverine inventory while nitrification alters the isotope compositions. In the coastal zone that receives the Changjiang River runoff, when salinities <20, positive offsets for NO_3^- concentration were obtained, likely due to the strong nitrification supplied by remineralization of N on particles and DON. The NO_3^- production peaked at the TMZ because of resuspension of particles and high levels of DO. In the high salinity CDW (salinity >20), the surface water became a sink for NO_3^- due to diatom assimilation. Consequently, 20 isohaline can be regarded as a boundary for the rapid uptake of nutrients by primary producers, benefiting the predication of algae bloom in coastal management. Compared with transect A, the strong stratification at the outer plume of transect B markedly stimulated phytoplankton utilization. The boost in the biological assimilation did not increase diatom biomass, therefore the assimilation may be linked to phytoplankton luxury consumption. In the bottom water, denitrification and nitrification coexisted. Nitrification was supplied by the degradation of algae debris, which increased NO_3^- concentrations but decreased stable isotope compositions. Denitrification likely occurred at the water-sediment interface that continuously removed NO_3^-, but without significant alternation on NO_3^- due to completed transformation. The production and removal for NO_3^- in the CDW should be taken into consideration by coastal managers and modeling workers. Furthermore, microorganism analyses and incubation experiments to quantitatively determine the dynamic between

environmental drivers and NO_3^- addition/removal rates are necessary.

6 DATA AVAILABILITY STATEMENT

The data used in the present study are available from the corresponding author upon request.

7 ACKNOWLEDGMENT

Technical support by Prof. GAO Yonghui, Prof. LI Bo, Ms. ZHENG Wei, Dr. ZHU Xunchi, Ms. QI Lijun, Mr. LIU Zhengbo, Ms. CAO Wanwan, Ms. JIANG Shuo, Mr. ZHU Kun, Mr. DAI Jinlong, and the R/V *Zheyuke II* crew during the cruise are acknowledged. The authors also appreciate the great assistance from Prof. YU Zhiming at the Institute of Oceanology, Chinese Academy of Sciences for the assistance in stable isotope analyses. Thanks are also due to the editor and anonymous reviewers, whose comments helped to improve the original manuscript.

References

Bowes M J, Ings N L, McCall S J, Warwick A, Barrett C, Wickham H D, Harman S A, Armstrong L K, Scarlett P M, Roberts C, Lehmann K, Sing A C. 2012. Nutrient and light limitation of periphyton in the River Thames: implications for catchment management. *Science of the Total Environment*, **434**: 201-212, https://doi.org/10.1016/j.scitotenv.2011.09.082.

Cai P H, Shi X M, Hong Q Q, Li Q, Liu L F, Guo X H, Dai M H. 2015. Using $^{224}Ra/^{228}Th$ disequilibrium to quantify benthic fluxes of dissolved inorganic carbon and nutrients into the Pearl River Estuary. *Geochimica et Cosmochimica Acta*, **170**: 188-203, https://doi.org/10.1016/j.gca.2015.08.015.

Casciotti K L, McIlvin M R. 2007. Isotopic analyses of nitrate and nitrite from reference mixtures and application to Eastern Tropical North Pacific waters. *Marine Chemistry*, **107**(2): 184-201, https://doi.org/10.1016/j.marchem.2007.06.021.

Chang C C Y, Kendall C, Silva S R, Battaglin W A, Campbell D H. 2002. Nitrate stable isotopes: tools for determining nitrate sources among different land uses in the Mississippi River Basin. *Canadian Journal of Fisheries and Aquatic Sciences*, **59**(12): 1 874-1 885, https://doi.org/10.1139/f02-153.

Chang P H, Isobe A, Kang K R, Ryoo S B, Kang H S, Kim Y H. 2014. Summer behavior of the Changjiang diluted water to the East/Japan Sea: a modeling study in 2003. *Continental Shelf Research*, **81**: 7-18, https://doi.org/10.1016/j.csr.2014.03.007.

Chen F J, Jia G D, Chen J Y. 2009. Nitrate sources and watershed denitrification inferred from nitrate dual isotopes in the Beijiang River, South China. *Biogeochemistry*, **94**(2): 163-174, https://doi.org/10.1007/s10533-009-9316-x.

Codispoti L A, Christensen J P. 1985. Nitrification, denitrification and nitrous oxide cycling in the eastern tropical South Pacific Ocean. *Marine Chemistry*, **16**(4): 277-300, https://doi.org/10.1016/0304-4203(85)90051-9.

Collos Y, Siddiqi M Y, Wang M Y, Glass A D M, Harrison P J. 1992. Nitrate uptake kinetics by two marine diatoms using the radioactive tracer ^{13}N. *Journal of Experimental Marine Biology and Ecology*, **163**(2): 251-260, https://doi.org/10.1016/0022-0981(92)90053-D.

Dai Z J, Du J Z, Zhang X L, Su N, Li J F. 2011. Variation of riverine material loads and environmental consequences on the Changjiang (Yangtze) estuary in recent decades (1955−2008). *Environmental Science & Technology*, **45**(1): 223-227, https://doi.org/10.1021/es103026a.

Domangue R J, Mortazavi B. 2018. Nitrate reduction pathways in the presence of excess nitrogen in a shallow eutrophic estuary. *Environmental Pollution*, **238**: 599-606, https://doi.org/10.1016/j.envpol.2018.03.033.

Ebina J, Tsutsui T, Shirai T. 1983. Simultaneous determination of total nitrogen and total phosphorus in water using peroxodisulfate oxidation. *Water Research*, **17**(12): 1 721-1 726, https://doi.org/10.1016/0043-1354(83)90192-6.

Edmond J M, Spivack A, Grant B C, Hu M H, Chen Z, Chen S, Zeng X. 1985. Chemical dynamics of the Changjiang Estuary. *Continental Shelf Research*, **4**(1-2): 17-36, https://doi.org/10.1016/0278-4343(85)90019-6.

Eyre B. 1994. Nutrient biogeochemistry in the tropical Moresby River Estuary system North Queensland, Australia. *Estuarine*, *Coastal and Shelf Science*, **39**(1): 15-31, https://doi.org/10.1006/ecss.1994.1046.

Galloway J N, Dentener F J, Capone D G, Boyer E W, Howarth R W, Seitzinger S P, Asner G P, Cleveland C C, Green P A, Holland E A, Karl D M, Michaels A F, Porter J H, Townsend A R, Vöosmarty C J. 2004. Nitrogen cycles: past, present, and future. *Biogeochemistry*, **70**(2): 153-226, https://doi.org/10.1007/s10533-004-0370-0.

Gao L, Li D J, Zhang Y W. 2012. Nutrients and particulate organic matter discharged by the Changjiang (Yangtze River): seasonal variations and temporal trends. *Journal of Geophysical Research-Biogeosciences*, **117**(G4): G04001, https://doi.org/10.1029/2012JG001952.

Gao X L, Song J M. 2005. Phytoplankton distributions and their relationship with the environment in the Changjiang Estuary, China. *Marine Pollution Bulletin*, **50**(3): 327-335, https://doi.org/10.1016/j.marpolbul.2004.11.004.

Granger J, Sigman D M, Rohde M M, Maldonado M T, Tortell P D. 2010. N and O isotope effects during nitrate assimilation by unicellular prokaryotic and eukaryotic plankton cultures. *Geochimica et Cosmochimica Acta*, **74**(3): 1 030-1 040, https://doi.org/10.1016/j.gca.2009.10.044.

Hansen H P, Koroleff F. 1999. Determination of nutrients. *In*: Grasshoff K, Kremling K, Ehrhardt M eds. Methods of Seawater Analysis. Wiley, Washington. p.159-228.

Hsiao S S Y, Hsu T C, Liu J W, Xie X, Zhang Y, Lin J, Wang H, Yang J Y T, Hsu S C, Dai M, Kao S J. 2014. Nitrification and its oxygen consumption along the turbid Chang Jiang River plume. *Biogeosciences*, **11**(7): 2 083-2 098, https://doi.org/10.5194/bg-11-2083-2014.

Huang J K, Hu R F, Cao J M, Rozelle S. 2008. Training

programs and in-the-field guidance to reduce China's overuse of fertilizer without hurting profitability. *Journal of Soil and Water Conservation*, **63**(5): 165A-167A, https://doi.org/10.2489/jswc.63.5.165A.

Jiang S, Müller M, Jin J, Wu Y, Zhu K, Zhang G S, Mujahid A, Rixen T, Muhamad M F, Sia E S A, Jang F H A, Zhang J. 2019. Dissolved inorganic nitrogen in a tropical estuary in Malaysia: transport and transformation. *Biogeosciences*, **16**(14): 2 821-2 836, https://doi.org/10.5194/bg-16-2821-2019.

Justić D, Turner R E, Rabalais N N. 2003. Climatic influences on riverine nitrate flux: implications for coastal marine eutrophication and hypoxia. *Estuaries*, **26**(1): 1-11, https://doi.org/10.1007/BF02691688.

Ketchum B H. 1939. The absorption of phosphate and nitrate by illuminated cultures of *Nitzschia closterium*. *American Journal of Botany*, **26**(6): 399-407, https://doi.org/10.1002/j.1537-2197.1939.tb09293.x.

Kuypers M M M, Marchant H K, Kartal B. 2018. The microbial nitrogen-cycling network. *Nature Reviews Microbiology*, **16**(5): 263-276, https://doi.org/10.1038/nrmicro.2018.9.

Kuypers M M M. 2017. Microbiology: a fight for scraps of ammonia. *Nature*, **549**(7671): 162-163, https://doi.org/10.1038/549162a.

Li S L, Liu C Q, Li J, Liu X L, Chetelat B, Wang B L, Wang F S. 2010. Assessment of the sources of nitrate in the Changjiang River, China using a nitrogen and oxygen isotopic approach. *Environmental Science & Technology*, **44**(5): 1 573-1 578, https://doi.org/10.1021/es902670n.

Li Z, Song S Q, Li C W, Yu Z M. 2018. The sinking of the phytoplankton community and its contribution to seasonal hypoxia in the Changjiang (Yangtze River) estuary and its adjacent waters. *Estuarine*, *Coastal and Shelf Science*, **208**: 170-179, https://doi.org/10.1016/j.ecss.2018.05.007.

Liu S M, Qi X H, Li X N, Ye H R, Wu Y, Ren J L, Zhang J, Xu W Y. 2016. Nutrient dynamics from the Changjiang (Yangtze River) estuary to the East China Sea. *Journal of Marine Systems*, **154**: 15-27, https://doi.org/10.1016/j.jmarsys.2015.05.010.

Liu X J, Yu Z M, Song X X, Cao X H. 2009. The nitrogen isotopic composition of dissolved nitrate in the Yangtze River (Changjiang) estuary, China. *Estuarine*, *Coastal and Shelf Science*, **85**(4): 641-650, https://doi.org/10.1016/j.ecss.2009.09.017.

Lohrenz S E, Fahnenstiel G L, Redalje D G, Lang G A, Dagg M J, Whitledge T E, Dortch Q. 1999. Nutrients, irradiance, and mixing as factors regulating primary production in coastal waters impacted by the Mississippi River plum. *Continental Shelf Research*, **19**(9): 1 113-1 141, https://doi.org/10.1016/S0278-4343(99)00012-6.

Loken L C, Small G E, Finlay J C, Sterner R W, Stanley E H. 2016. Nitrogen cycling in a freshwater estuary. *Biogeochemistry*, **127**(2-3): 199-216, https://doi.org/10.1007/s10533-015-0175-3.

Manna R K, Satpathy B B, Roshith C M, Naskar M, Bhaumik U, Sharma A P. 2013. Spatio-temporal changes of hydro-chemical parameters in the estuarine part of the River Ganges under altered hydrological regime and its impact on biotic communities. *Aquatic Ecosystem Health & Management*, **16**(4): 433-444, https://doi.org/10.1080/14634988.2013.853596.

Martens-Habbena W, Berube P M, Urakawa H, de la Torre J R, Stahl D A. 2009. Ammonia oxidation kinetics determine niche separation of nitrifying Archaea and Bacteria. *Nature*, **461**(7266): 976-979, https://doi.org/10.1038/nature08465.

Milliman J D, Farnsworth K L. 2011. River Discharge to the Coastal Ocean-A Global Synthesis. Cambridge University Press, London. 319p.

Moore W S. 2010. The effect of submarine groundwater discharge on the ocean. *Annual Review of Marine Science*, **2**: 59-88, https://doi.org/10.1146/annurev-marine-120308-081019.

Pennino M J, Kaushal S S, Murthy S N, Blomquist J D, Cornwell J C, Harris L A. 2016. Sources and transformations of anthropogenic nitrogen along an urban river-estuarine continuum. *Biogeosciences*, **13**(22): 6 211-6 228, https://doi.org/10.5194/bg-13-6211-2016.

Sanders T, Schöl A, Dähnke K. 2018. Hot spots of nitrification in the Elbe Estuary and their impact on nitrate regeneration. *Estuaries and Coasts*, **41**(1): 128-138, https://doi.org/10.1007/s12237-017-0264-8.

Santos M L S, Muniz K, Barros-Neto B, Araujo M. 2008. Nutrient and phytoplankton biomass in the Amazon River shelf waters. *Anais da Academia Brasileira de Ciências*, **80**(4): 703-717, https://doi.org/10.1590/S0001-37652008000400011.

Sebilo M, Billen G, Mayer B, Billiou D, Grably M, Garnier J, Mariotti A. 2006. Assessing nitrification and denitrification in the Seine River and estuary using chemical and isotopic techniques. *Ecosystems*, **9**(4): 564-577, https://doi.org/10.1007/s10021-006-0151-9.

Sigman D M, Casciotti K L, Andreani M, Barford C, Galanter M, Böhlke J K. 2001. A bacterial method for the nitrogen isotopic analysis of nitrate in seawater and freshwater. *Analytical Chemistry*, **73**(17): 4 145-4 153, https://doi.org/10.1021/ac010088e.

Song G D, Liu S M, Marchant H, Kuypers M M M, Lavik G. 2013. Anammox, denitrification and dissimilatory nitrate reduction to ammonium in the East China Sea sediment. *Biogeosciences*, **10**(11): 6 851-6 864, https://doi.org/10.5194/bg-10-6851-2013.

Thibodeau B, Hélie J F, Lehmann M F. 2013. Variations of the nitrate isotopic composition in the St. Lawrence River caused by seasonal changes in atmospheric nitrogen inputs. *Biogeochemistry*, **115**: 287-298, https://doi.org/10.1007/s10533-013-9834-4.

Wang W T, Yu Z M, Song X X, Wu Z X, Yuan Y Q, Zhou P, Cao X H. 2016. The effect of Kuroshio Current on nitrate dynamics in the southern East China Sea revealed by nitrate isotopic composition. *Journal of Geophysical Research: Oceans*, **121**(9): 7 073-7 087, https://doi.org/10.1002/2016JC011882.

Wang W T, Yu Z M, Song X X, Wu Z X, Yuan Y Q, Zhou P, Cao

X H. 2017. Characteristics of the $\delta^{15}NNO_3$ distribution and its drivers in the Changjiang River estuary and adjacent waters. *Chinese Journal of Oceanology and Limnology*, **35**(2): 367-382, https://doi.org/10.1007/s00343-016-5276-x.

Wang W T, Yu Z M, Wu Z X, Song S Q, Song X X, Yuan Y Q, Cao X H. 2018. Rates of nitrification and nitrate assimilation in the Changjiang River estuary and adjacent waters based on the nitrogen isotope dilution method. *Continental Shelf Research*, **163**: 35-43, https://doi.org/10.1016/j.csr.2018.04.014.

Weigand M A, Foriel J, Barnett B, Oleynik S, Sigman D M. 2016. Updates to instrumentation and protocols for isotopic analysis of nitrate by the denitrifier method. *Rapid Communications in Mass Spectrometry*, **30**(12): 1 365-1 383, https://doi.org/10.1002/rcm.7570.

Wong W W, Grace M R, Cartwright I, Cook P L M. 2014. Sources and fate of nitrate in a groundwater-fed estuary elucidated using stable isotope ratios of nitrogen and oxygen. *Limnology and Oceanography*, **59**(5): 1 493-1 509, https://doi.org/10.4319/lo.2014.59.5.1493.

Wu H, Zhu J R, Choi B H. 2010. Links between saltwater intrusion and subtidal circulation in the Changjiang Estuary: a model-guided study. *Continental Shelf Research*, **30**(17): 1 891-1 905, https://doi.org/10.1016/j.csr.2010.09.001.

Xue D M, Botte J, De Baets B, Accoe F, Nestler A, Taylor P, Van Cleemput O, Berglund M, Boeckx P. 2009. Present limitations and future prospects of stable isotope methods for nitrate source identification in surface- and groundwater. *Water Research*, **43**(5): 1 159-1 170, https://doi.org/10.1016/j.watres.2008.12.048.

Yan X L, Xu M N, Wan X S, Yang J Y T, Trull T W, Dai M H, Kao S J. 2017. Dual isotope measurements reveal zoning of nitrate processing in the summer Changjiang (Yangtze) river plume. *Geophysical Research Letters*, **44**(24): 12 289-12 297, https://doi.org/10.1002/2017GL075951.

Yang H J, Shen Z M, Zhang J P, Wang W H. 2007. Water quality characteristics along the course of the Huangpu River (China). *Journal of Environmental Sciences*, **19**(10): 1 193-1 198, https://doi.org/10.1016/S1001-0742(07)60195-8.

Yang Y P, Zhang M J, Li Y T, Zhang W. 2015. The variations of suspended sediment concentration in Yangtze River Estuary. *Journal of Hydrodynamics*, **27**(6): 845-856, https://doi.org/10.1016/s1001-6058(15)60547-9.

Yao Q Z, Yu Z G, Li L L, Chen HT, Mi T Z. 2014. Transformation and source of nutrients in the Changjiang Estuary. *Science China Chemistry*, **57**(5): 779-790, https://doi.org/10.1007/s11426-013-5040-4.

Yu H Y, Yu Z M, Song X X, Cao X H, Yuan Y Q, Lu G Y. 2015. Seasonal variations in the nitrogen isotopic composition of dissolved nitrate in the Changjiang River estuary, China. *Estuarine*, *Coastal and Shelf Science*, **155**: 148-155, https://doi.org/10.1016/j.ecss.2015.01.017.

Zhang A Y, Zhang J, Hu J, Zhang R F, Zhang G S. 2015. Silicon isotopic chemistry in the Changjiang Estuary and coastal regions: impacts of physical and biogeochemical processes on the transport of riverine dissolved silica. *Journal of Geophysical Research-Oceans*, **120**(10): 6 943-6 957, https://doi.org/10.1002/2015JC011050.

Zhang A. 2007. Study on the Controlling of Nutrient Phase Transformation by Adsorption-Desorption in the Chanjiang Estuary. East China Normal University, Shanghai, China. 168p.

Zhang J, Wu Y, Jennerjahn T C, Ittekkot V, He Q. 2007. Distribution of organic matter in the Changjiang (Yangtze River) Estuary and their stable carbon and nitrogen isotopic ratios: implications for source discrimination and sedimentary dynamics. *Marine Chemistry*, **106**(1-2): 111-126, https://doi.org/10.1016/j.marchem.2007.02.003.

Zhang J. 1996. Nutrient elements in large Chinese estuaries. *Continental Shelf Research*, **16**(8): 1 023-1 045, https://doi.org/10.1016/0278-4343(95)00055-0.

Zhu J R, Chen C S, Ding P X, Li C Y, Lin H C. 2004. Does the Taiwan warm current exist in winter? *Geophysical Research Letters*, **31**(12): L12302, https://doi.org/10.1029/2004gl019997.

Zhu X C, Zhang R F, Wu Y, Zhu J R, Bao D Y, Zhang J. 2018. The remobilization and removal of Fe in Estuary-a case study in the Changjiang Estuary, China. *Journal of Geophysical Research-Oceans*, **123**(4): 2 539-2 553, https://doi.org/10.1002/2017JC013671.

Electronic supplementary material

Supplementary material (Supplementary Tables S1–S4, Figs.S1–S3) is available in the online version of this article at https://doi.org/10.1007/s00343-020-0149-8.